



Everett, R. D. (2016) Dynamic response of IFI16 and promyelocytic leukemia nuclear body components to herpes simplex virus 1 infection. *Journal of Virology*, 90(1), pp. 167-179.

There may be differences between this version and the published version. You are advised to consult the publisher's version if you wish to cite from it.

<http://eprints.gla.ac.uk/114885/>

Deposited on: 19 February 2016

Enlighten – Research publications by members of the University of Glasgow
<http://eprints.gla.ac.uk>

1
2
3
4
5
6
7
8
9
10
11
12
13
14
15
16
17
18
19
20
21
22
23
24
25
26
27

The dynamic response of IFI16 and PML Nuclear Body components to HSV-1 infection.

Roger D. Everett

MRC - University of Glasgow Centre for Virus Research, University of Glasgow Scotland,
U.K.

Running Head: Dynamic response of IFI16 to HSV-1 infection

Address correspondence to Roger Everett, roger.everett@glasgow.ac.uk

Key words: HSV-1, ICP0, IFI16, PML, hDaxx

Abstract word count: 250

Main text word count (excluding references, tables and Fig. legends): 5925

28 **Abstract**

29 Intrinsic immunity is an aspect of antiviral defence that operates through diverse mechanisms
30 at the intracellular level through a wide range of constitutively expressed cellular proteins. In
31 the case of herpesviruses, intrinsic resistance involves the repression of viral gene expression
32 during the very early stages of infection, a process that is normally overcome by viral
33 tegument and/or immediate-early proteins. Thus the balance between cellular repressors and
34 viral counteracting proteins determines whether or not a cell becomes productively infected.
35 One aspect of intrinsic resistance to herpes simplex virus type 1 (HSV-1) is conferred by
36 components of PML Nuclear Bodies, which respond to infection by accumulating at sites that
37 are closely associated with the incoming parental HSV-1 genomes. Other cellular proteins
38 also respond to viral genomes in this manner, including IFI16 which has been implicated in
39 sensing pathogen DNA and initiating signalling pathways that lead to an interferon response.
40 Here, studies of the dynamics of the response of PML NB components and IFI16 to invading
41 HSV-1 genomes demonstrate that this response is extremely rapid, occurring within the first
42 hour after addition of the virus, and that hDaxx and IFI16 respond more rapidly than PML. In
43 the absence of HSV-1 regulatory protein ICP0, which counteracts the recruitment process, the
44 newly formed, viral genome induced PML NB-like foci can fuse with existing PML NBs.
45 These data are consistent with a model involving viral genome sequestration into such
46 structures thereby contributing to the low probability of initiation of lytic infection in the
47 absence of ICP0.

48

49 **Importance**

50 Herpesviruses have intimate interactions with their hosts, with infection leading either to the
51 productive lytic cycle or to a quiescent infection in which viral gene expression is suppressed
52 while the viral genome is maintained in the host cell nucleus. Whether a cell becomes
53 lytically or quiescently infected can be determined through the competing activities of
54 cellular repressors and viral activators, some of which counteract cell mediated repression.
55 Therefore the events that occur within the earliest stages of infection can be of crucial
56 importance. Using live cell microscopy, this paper describes the extremely rapid response to
57 herpes simplex virus type 1 infection of the cellular protein IFI16, a sensor of pathogen DNA,
58 and also the PML Nuclear Body proteins PML and hDaxx. The data imply that these proteins
59 can accumulate on or close to the viral genomes in a sequential manner which may lead to
60 their sequestration and repression.

61 **INTRODUCTION**

62 Whether or not a cell becomes productively infected with herpes simplex virus type 1 (HSV-
63 1), as with other herpesviruses, depends on many factors that modulate the initial stages of
64 infection. Amongst these are cellular proteins that respond in a restrictive manner to repress
65 viral gene expression once the viral genomes have entered the nucleus, while the virus
66 expresses proteins that counteract these repressive effects or stimulate viral gene expression
67 more directly. Over the last decade, it has become clear that one class of restricting cellular
68 factors comprises a number of components of promyelocytic leukaemia (PML) Nuclear
69 Bodies (PML NBs, also known as ND10), including PML itself, Sp100, hDaxx and ATRX
70 (reviewed in (1-3)). The HSV-1 Immediate-Early protein ICP0 is responsible for overcoming
71 restriction mediated by these proteins through mechanisms that require its E3 ubiquitin ligase
72 activity (reviewed in (1)). HSV-1 mutants that are unable to express active ICP0 have a very
73 low probability of initiating lytic infection in restrictive cell types (4-6), but are able to
74 replicate more efficiently in cells depleted of one or more of these PML NB proteins (7-10).

75 There is considerable evidence that the restrictive effects of PML NB components
76 depend on their dynamic response to infection. PML, Sp100 and hDaxx are recruited to sites
77 that are closely associated with HSV-1 genomes during the earliest stages of infection (11,
78 12) by mechanisms that involve sumoylation and/or their ability to interact with sumoylated
79 proteins, and which are inhibited by ICP0 (7-9, 13). It is likely that other cellular proteins that
80 accumulate on or near HSV-1 genomes in a SUMO pathway dependent manner will be
81 identified in the future, and because ICP0 causes a wide ranging reduction in the levels of
82 sumoylated species during infection (14-16) their recruitment may also be sensitive to ICP0.
83 Interestingly, although PML is required for the assembly of PML NBs in uninfected cells (17,
84 18) it is not required for recruitment of either hDaxx or Sp100 to viral genomes, and indeed
85 these proteins may be recruited independently (7-9). Recruitment defective mutants of PML
86 and hDaxx, unlike their wild type counterparts, are unable to reverse the stimulatory effects
87 on ICP0 null mutant HSV-1 replication of shRNA mediated knock-down of the endogenous
88 proteins (9, 13, 19).

89 The signals that initiate the recruitment of PML NB components to HSV-1 genomes
90 remain unknown. It is possible that it is related to a DNA repair response, and indeed several
91 DNA repair proteins respond to infection in a similar manner (20), but recruitment of PML
92 still occurs in DNA repair deficient cells (20). More recently, the cellular DNA sensor IFI16
93 (21, 22) has also been implicated in the initiation of pathways that are inhibitory to HSV-1,
94 either through initiating events leading to an interferon response (22, 23) or more direct

95 effects on viral gene expression (24-27). ICP0 null mutant HSV-1 has an increased plaque
96 forming potential in cells depleted of IFI16 (24, 26). IFI16 is degraded during HSV-1
97 infection by a mechanism that was originally thought to be ICP0-dependent (23), although
98 later work showed that ICP0 was neither sufficient nor necessary for this degradation (24,
99 28). Indeed, cellular factors (and cell type) also contribute to the stability of IFI16 during
100 HSV-1 infection (24, 25, 27). Nonetheless during a normal experimental infection IFI16 is
101 degraded more rapidly during a wild type (wt) than an ICP0 null mutant infection, unless the
102 latter is conducted at very high multiplicity. Like the PML NB components, IFI16 also
103 localizes to HSV-1 genomes during the early stages of infection (23-29), and ICP0 inhibits
104 this process (24).

105 In order to study the dynamic responses of this group of cellular proteins during the
106 very earliest stages of HSV-1 infection, analyses were conducted in live cells expressing near
107 endogenous levels of PML, hDaxx or IFI16, or combinations thereof, tagged with EYFP,
108 ECFP or a dual fusion protein that expresses red fluorescence constitutively and in addition
109 green fluorescence after photoactivation. These studies revealed the extremely rapid and in
110 some cases transient responses of these proteins during HSV-1 infection. Within the first hour
111 after addition of the virus, IFI16 was observed to form distinct but highly transient foci that
112 are almost certainly associated with HSV-1 genomes. This occurred with both wt and ICP0-
113 null mutant viruses, but in the latter case a second and more stable phase of recruitment of
114 IFI16 was observed. Recruitment of IFI16 to HSV-1 genomes was observed with equal
115 efficiency in PML-depleted cells. Efficient recruitment of hDaxx to these foci also occurred
116 very rapidly, but that of PML took place more slowly. These events occur in both wt and
117 ICP0 null mutant infections, but were very transient in the former, presumably because of the
118 effects of ICP0. Photoactivation experiments illustrated that hDaxx molecules in one part of
119 the cell nucleus could be recruited to viral genomes in the opposite half of the nucleus within
120 seconds. These studies reveal highly dynamic and in some cases sequential or transient events
121 of cellular protein recruitment to HSV-1 genomes that would not be amenable to study by
122 fixed cell methods. Importantly, the results reveal that the cell responds to the entry of viral
123 genomes into the nucleus certainly within minutes and probably within seconds, long before a
124 cell can be detected as being infected through the production of viral proteins.

125 **MATERIALS AND METHODS**

126 **Viruses and cells**

127 HSV-1 strain 17+ was the wt strain used, from which the ICP0-null mutant *dl1403* was
128 derived (5). Virus *dl0C4*, a derivative of *dl1403* that expresses ECFP-linked ICP4, was
129 constructed as described (4). All viruses were grown in BHK cells and titrated in U2OS cells,
130 in which ICP0 is not required for efficient HSV-1 replication (6). Human diploid fibroblasts
131 (HFs), PML-depleted HFs (7), telomerase immortalized HFs (HFTs, a gift from Chris
132 Boutell), U2OS and HEK-293T cells were grown in Dulbecco's Modified Eagles' Medium
133 supplemented with 10% fetal calf serum (FCS). BHK cells were grown in Glasgow Modified
134 Eagles' Medium supplemented with 10% new born calf serum and 10% tryptose phosphate
135 broth. HepaRG cells were grown in William's Medium E supplemented with 10% fetal
136 bovine serum Gold (PAA Laboratories Ltd), 2 mM glutamine, 5 µg/ml insulin and 500 nM
137 hydrocortisone. All cell growth media were supplemented with 100 units/ml penicillin and
138 0.1 mg/ml streptomycin. Lentivirus transduced cells were maintained with continuous
139 antibiotic selection, as appropriate.

140 **Lentiviral vectors**

141 Lentiviral vectors expressing EYFP-linked PML isoform I or hDaxx from the weak HSV-1
142 glycoprotein D promoter and including G418 resistance have been described previously (9,
143 13, 19). Derivatives of these were constructed in which the G418 resistance marker was
144 replaced by puromycin resistance, while versions were also constructed in which ECFP was
145 used in place of EYFP. The same backbone was used to express EYFP-linked IFI16 using a
146 cDNA purchased from Origene. IFI16 mutant m3 (S27A/L28A/D50A; (30)) was constructed
147 by replacement of the wt cDNA with the complete m3 cDNA made by PCR from a plasmid
148 supplied by Jungsan Sohn. Derivative Δ HIN2 which lacks IFI16 codons 518 – 729 was
149 constructed by PCR splicing and replacement of the wt sequence. Lentiviral vectors
150 expressing PML isoform I or hDaxx linked to a fusion of photoactivatable EGFP and
151 constitutively fluorescent mCherry were constructed by replacement of the EYFP coding
152 region of vectors pLNGY-PML.I and pLNGY-hDaxx with the dual fluorescent (GAPC)
153 cassette (31). Lentivirus transduction, selection of transduced cells and maintenance of cell
154 lines were as described previously (7). Sequential transduction was used to prepare cells
155 expressing EYFP-IFI16 with either ECFP-hDaxx or ECFP-PML, or EYFP-hDaxx with
156 ECFP-PML. Selection during routine culture used G418 at 0.5 mg/ml and/or puromycin at
157 500 ng/ml as relevant. The antibiotic was omitted from cells seeded for and during
158 experimentation.

159 **Antibodies**

160 The following antibodies were used: anti-actin mAb AC-40 (Sigma-Aldrich), anti-PML
161 rabbit polyclonal (rAb) ABD030 (Jena Bioscience) or mAb 5E10 (32), anti-IFI16 mAb
162 ab55328 (Abcam), anti-hDaxx rAb 07-471 (Upstate), anti-ICP4 mAb 58S (33) and anti-
163 EGFP rAb ab290 (Abcam).

164 **Immunofluorescence**

165 Cells on 13 mm glass coverslips were fixed with formaldehyde and prepared for
166 immunofluorescence using standard methods. The secondary antibodies used were FITC-
167 conjugated sheep anti-mouse IgG (Sigma), Alexa 555 conjugated goat anti-mouse or anti-
168 rabbit IgG and Alexa 633 conjugated goat anti-rabbit IgG (Invitrogen). The samples were
169 examined using a Zeiss LSM 710 confocal microscope, with 488 nm, 561 nm and 633 nm
170 laser lines, scanning each channel separately under image capture conditions that eliminated
171 channel overlap. The images were exported as tif files, minimally adjusted using Photoshop,
172 then assembled into the figures using Illustrator.

173 **Live cell microscopy**

174 Cells were seeded into Nunc Lab-Tec chambered coverglass live cell chambers at 1×10^5
175 cells per well (4 chambered unit) then infected or not as relevant the following day.
176 Immediately prior to infection the cells were washed with DMEM without phenol red, and
177 after virus adsorption they were overlaid with the same medium containing 2% FCS and
178 antibiotics as above. For high multiplicity of infection (MOI) experiments, a range of MOI
179 between 25 and 100 was used. The nature of the results was not essentially influenced by
180 choice of MOI, except that events occurred more commonly and were thus easier to detect as
181 the MOI was increased. If plaques were later to be examined, the medium in the overlay also
182 included 1% human serum. If the cells were to be examined immediately, the virus
183 absorption period was 15 minutes, then the cells were placed into the microscope incubation
184 chamber (pre-heated to 37 °C) and imaging was commenced as soon as possible. In this latter
185 case, times stated in the figures relate to time after addition of the virus. The microscope was
186 a Zeiss Axio Observer Z1 equipped with definite focus control to maintain the correct focal
187 plane during a time course. The S1 environmental system was used to maintain CO₂ at 5%
188 and temperature and humidity. Filter sets 47 HE and 46 HE were used for detecting ECFP
189 and EYFP respectively, using illumination from an HXP 120V unit. The samples were
190 examined using either x40 NA 1.3 or x63 NA 1.4 oil immersion lenses. Image capture
191 conditions generally utilised 70% or 50% HXP power with 2x gain and 4x4 binning, with
192 exposure times of the order of 100 – 200 ms for both channels. The time intervals between

193 images are noted in each figure as relevant. Imaging conditions were adjusted so that the cells
194 did not suffer detectably from light poisoning and so that any photobleaching was minimized
195 during the course of the experiment. Generally this was not a problem for EYFP-IFI16 or
196 ECFP-PML, but ECFP-hDaxx gave weaker fluorescence and was subject to photobleaching
197 if image capture frequency or illumination intensity was too high. Cells were selected for
198 imaging on the basis of signal intensities to ensure sufficient image quality. For IFI16 this
199 was fairly uniform, but cells expressing sufficient ECFP-hDaxx were in a minority.
200 Relevant segments of the image series were cropped and exported as avi files (for the
201 Supplemental movies) or saved separately for excision of individual frames for presentation
202 in the figures, after adjustment of minimum and maximum thresholds for each channel for
203 ease of visualization. Due to space constraints, only a small number of examples of each
204 phenomenon can be presented in the figures. In some cases, additional events of the same
205 nature can be seen in the accompanying Supplemental Movies (which may cover a longer
206 time frame). In all cases, the data presented are representative of several independent
207 experiments.

208 For the photoactivation experiments, cells were examined in a live cell adapted Zeiss
209 LSM 510 META microscope with incubation at 37°C and 5% CO₂. Selected cells were first
210 imaged for mCherry, then regions of interest were illuminated with the 405 nm laser at 50%
211 power for 10 reiterations using the bleach programme in the LSM 510 software. Subsequent
212 imaging was performed at timed intervals thereafter for both EGFP and mCherry using the
213 488 nm and 543 nm lasers respectively. For GAPC-hDaxx, images were acquired at 2 second
214 intervals after bleaching, while 15 second intervals were used for GAPC-PML.I.

215

216 **RESULTS**

217 **Description of the basic experimental system and underlying assumptions and** 218 **extrapolations**

219 Gerd Maul was first to observe that the genomes of many DNA viruses, particularly HSV-1
220 and HCMV, could be observed to be in association with PML NBs during the early stages of
221 infection (34, 35). These studies used the difficult technique of fluorescence in situ
222 hybridisation (FISH) to detect the viral genomes, which although providing direct evidence,
223 is limited because antibody staining techniques to detect viral or cellular proteins are not
224 always compatible with the required harshness of the hybridisation procedure. Later it was
225 discovered that in cells at the edges of developing plaques, viral genomes could be detected
226 frequently in large numbers of foci that formed characteristic arcs just inside the nuclear

227 envelope. These genomes could be detected by FISH, but also importantly by simple
228 fluorescence detection of the viral transcriptional activator protein ICP4 (11). This occurs
229 because ICP4 binds avidly to viral DNA. Thus in such cells an asymmetric pattern of ICP4
230 foci near the nuclear periphery could be taken to identify viral genome sites, without the need
231 for FISH. Because this highly asymmetric staining pattern is completely distinct from the
232 normal situation in uninfected cells, it can be safely deduced that PML NB protein foci in this
233 arrangement are also associated with the mutant viral genomes, even if neither FISH nor
234 ICP4 staining are included in the protocol. Several experiments in this report are dependent
235 on this deduction. Analogous recruitment can also be observed in wt HSV-1 infections, but
236 this is difficult to detect because the effects of ICP0 render it weak and transient (11). Having
237 established these facts, it becomes possible to infer that small novel foci of relevant cellular
238 proteins that can be detected only after a cell is infected are also highly likely to be associated
239 with viral genomes. This is an important extrapolation in a number of the following
240 experiments, but it is also supported by additional data where possible. These reasonable
241 deductions and extrapolations are necessary because it is not possible to utilise FISH in live
242 cells, and it is sometimes difficult to combine an experimental protocol with the use of a virus
243 expressing fluorescently tagged ICP4. As examples of these phenomena, various phenotypes
244 of PML and hDaxx recruited to ICP4 foci in cells at the edge of a developing ICP0 null
245 mutant plaque are presented in Fig. 1, and for IFI16 in Fig. 2.

246 **The pyrin domain of IFI16 is required for its recruitment to HSV-1 genomes**

247 We and others have observed that IFI16 is also recruited efficiently to HSV-1 genomes at the
248 early stages of infection (23-29). In order to study this in more detail, we used a lentiviral
249 vector system for expressing EYFP-tagged IFI16 (Fig. 2A). Transduced human fibroblasts
250 were selected with G418 then EYFP-positive cells were enriched by FACS. Analysis of the
251 resultant cell line by western blotting showed that the cells expressed EYFP-linked IFI16 at
252 levels of the same order as the three endogenous isoforms (Fig. 2B). We used the same
253 system to express two mutant forms of IFI16, one with three point mutations in the pyrin
254 domain (mutant m3) (30) and one a deletion of the second DNA binding HIN domain
255 (Δ HIN2) (Fig. 2C). The EYFP-IFI16 proteins expressed in these cell lines were distributed
256 similarly in the nucleus, with a general diffuse signal throughout the nucleoplasm and a
257 concentration in the nucleoli (Fig. 2D). This is very similar to endogenous IFI16 in HFs (24,
258 26). As with the endogenous protein (24), wt EYFP-IFI16 was clearly recruited to sites
259 associated with HSV-1 genomes (detected by ICP4) in cells at the edge of developing ICP0
260 null mutant plaques (Fig. 2E, upper row). This recruitment is not detectable in this way in wt

261 infected cells because of ICP0 activity (24). The recruitment of EYFP-IFI16 also occurred
262 normally in the case of the Δ HIN2 mutant (Fig. 2E, bottom row), showing that one DNA
263 binding HIN domain is sufficient for this activity, but the PYD mutant m3 was not efficiently
264 recruited (Fig. 2E, middle row). The pyrin domain is required for oligomerization of IFI16
265 when bound to DNA (30), and therefore the recruitment of IFI16 probably represents
266 assembly of IFI16 oligomers on the viral DNA at this stage of infection, soon after it is
267 released into the nucleus in an unchromatinised form. It was not possible to test whether
268 deletion of both HIN domains also inhibited recruitment as further deletion upstream of HIN2
269 caused loss of expression in this system.

270 **Depletion of PML does not compromise recruitment of IFI16 to HSV-1 genomes**

271 It was of interest to determine whether or not PML is involved in the recruitment of IFI16 to
272 HSV-1 genomes. HF cells depleted of PML using a lentiviral shRNA vector (7) were infected
273 with ICP0 null mutant HSV-1 and the distributions of hDaxx and IFI16 in cells at the edges
274 of developing plaques were investigated. Infected cells could be identified by the
275 characteristic redistribution of hDaxx (see Fig. 1), and as expected IFI16 was similarly re-
276 distributed in such cells (Fig. 2F, left). The same distributions of hDaxx and IFI16 were
277 observed in infected PML depleted cells, while in uninfected cells hDaxx was dispersed
278 throughout the nucleoplasm (Fig. 2F, right). These data demonstrate that while PML is
279 required for hDaxx to be present in PML NB foci in uninfected cells (as reported previously;
280 (17, 18)), PML depletion compromises recruitment of neither hDaxx (in agreement with
281 previous data; (8)) nor IFI16. Thus recruitment of IFI16 to HSV-1 genomes is independent of
282 the events that lead to the transient co-localization of IFI16 with PML during the early stages
283 of wt HSV-1 infection (23, 24).

284 **Rapid response of IFI16 to HSV-1 genomes as they enter the nucleus**

285 Having developed a cell line expressing EYFP-linked wt IFI16, it was now possible to
286 examine the behaviour of the protein in live infected cells. An unexpected observation was
287 that high multiplicity ICP0 null mutant HSV-1 infection induced the formation of small,
288 discrete novel IFI16 foci, often just inside the nuclear periphery. These were highly transient,
289 in that they could appear and then disappear within 5 minutes, with others subsequently
290 appearing similarly in a different part of the cell (Fig. 3A and Supplemental Movie 1). Such
291 events also occurred during wt HSV-1 infection (Fig. 3B and Supplemental Movie 2). The
292 appearance of these foci was completely dependent on infection, and generally occurred
293 within the first hour or two after addition of the virus to the cell monolayer. Given their size
294 and location, it seemed possible that they represent transient recruitment of IFI16 onto HSV-1

295 genomes at the time and point that they are released into the nucleus. Support for this
296 explanation came from study of cells at the edge of a developing ICP0 null mutant plaque.
297 Such cells will be infected at much higher multiplicity than can be achieved by adding a virus
298 inoculum to the cell monolayer, and would thus be expected to display more of such foci.
299 This was indeed the case, with many examples of such transient foci being plainly visible in
300 Fig. 3C and Supplemental Movie 3.

301 Further support for this hypothesis came from infection of HF cells expressing EYFP-
302 IFI16 with dl0C4, an ICP0 null mutant HSV-1 expressing ECFP-linked ICP4 (4). The
303 compilation in Fig. 3D and Supplemental Movie 4 shows a cell at the edge of a developing
304 plaque from an image sequence that began before any IFI16 foci were detected. The
305 displayed images illustrate the appearance of transient IFI16 foci at various locations within
306 the first 42 minutes, mostly in the lower left quadrant of the cell but also elsewhere. As time
307 continues, the foci in this region become more stable and prominent, and develop into an arc-
308 like mass. The ECFP signal indicates that these apparently more stable IFI16 accumulations
309 are very close to where ICP4 foci begin to accumulate, marking the positions of viral
310 genomes. These data are consistent with the interpretation that this cell is being infected by
311 genomes arriving mostly in the lower left quadrant of the nucleus which initially induce
312 transient foci of IFI16. As infection develops, and ICP4 expression becomes detectable (and
313 likely DNA replication begins, as judged from the expansion of the ICP4 compartments), the
314 accumulations of IFI16 become more marked and longer lasting. From previous results, it can
315 also be deduced that this second phase is inhibited by ICP0, but the first phase takes place too
316 rapidly for it to be inhibited as it probably occurs before ICP0 is expressed in sufficient
317 quantities.

318 **Rapid recruitment of hDaxx from the nucleoplasm to HSV-1 genomes**

319 Previous work using fluorescence recovery after photobleaching (FRAP) had demonstrated
320 that hDaxx is highly mobile in the nucleus, with an exchange rate between PML NBs and the
321 general nucleoplasm measured in terms of seconds, while that for PML was slower but still in
322 the low numbers of minutes (11, 36-38). It had previously been suggested that this dynamics
323 behaviour would enable the formation of novel PML NB-like foci in association with HSV-1
324 genomes without the need for movement of pre-existing PML NBs (11). To address this point
325 further, lentiviral vectors were constructed that express either hDaxx or PML linked to a
326 fusion protein that includes mCherry and a photoactivatable version of EGFP (31). Thus the
327 expressed proteins are constitutively red fluorescent, but also are green fluorescent after
328 photoactivation by pulses of a 405 nm laser. In this way, the movement of molecules from

329 activated to unactivated parts of the nucleus could be monitored. This technique was
330 therefore adopted to examine the dynamics of recruitment of both hDaxx and PML from one
331 region of the nucleus to another in which viral genome foci were present. Experiments in
332 uninfected cells illustrated that photoactivation of both the PML and hDaxx fusion proteins
333 occurred as expected, and subsequently the migration of activated molecules to the
334 unactivated part of the nucleus could be observed. In the case of PML, this took place over a
335 period of minutes, while with hDaxx the timescale was in seconds, to the extent that some
336 transfer into the unactivated part of the nucleus was seen as soon as an image could be
337 captured after photoactivation (Fig. 4A). These results are consistent with the previous FRAP
338 experiments (11, 36-38). By applying this technique to cells at the edge of developing ICP0
339 null mutant HSV-1 plaques, characteristic recruited patterns of hDaxx and PML could be
340 seen via the mCherry fluorescence. After photoactivation of molecules in the opposite part of
341 the nucleus, the presence of activated hDaxx in the viral genome associated foci could be
342 detected at the earliest possible time point, becoming more pronounced within 15 seconds
343 (Fig. 4B, upper row). The same occurred with PML over a longer time course (Fig. 4B, lower
344 row). Therefore recruitment of hDaxx in particular to viral genome associated foci is
345 extremely rapid.

346 **IFI16 and hDaxx respond to HSV-1 genomes more rapidly than PML**

347 Given that both IFI16 and hDaxx can be recruited very rapidly to sites associated with HSV-1
348 genomes, it was of interest to determine whether a temporal order of IFI16 and PML NB
349 components could be determined. Therefore cells were constructed that express EYFP-IFI16
350 and either ECFP linked hDaxx or PML. The EYFP-IFI16/ECFP-hDaxx cells were infected at
351 high multiplicity with ICP0 null mutant HSV-1 then an image sequence was captured during
352 the very early stages of infection (Fig. 5). As before, in a proportion of cells transient virus-
353 induced small foci of IFI16 appeared, to which hDaxx was also recruited *de novo* either at the
354 same time point or very shortly thereafter. Therefore these proteins respond with similar
355 kinetics to HSV-1 infection. That hDaxx is also recruited to these novel, virus-induced IFI16
356 foci is further evidence that they are associated with viral genomes because it has been
357 established that hDaxx responds in this manner. As time proceeds, the IFI16 signal is lost
358 from these foci but they remain hDaxx positive.

359 A similar experiment was performed using EYFP-IFI16/ECFP-PML cells infected
360 with ICP0 null mutant HSV-1. Fig. 6 shows a cell infected at high MOI in which an example
361 of an event that commonly occurs in such cells was observed. First, a small accumulation of
362 IFI16 appears near the nuclear periphery which at this point contains no detectable PML (Fig.

363 6, 3 min time point). As before IFI16 appears only transiently, but at the 7 min time point this
364 dot also contains PML. At later time points, IFI16 is no longer detectable in this dot, while
365 PML remains in this novel focus. Over the following minutes the new PML dot becomes
366 closer to a pre-existing PML NB and then appears to merge with it. The top three rows of Fig.
367 6 show the IFI16, PML and merged signals of the cell in question over an 11 minute period,
368 while the lower three panels show enlargements of these images covering the event in
369 question. Examination of similar times over a longer period indicated that these events were
370 quite common, although the novel foci did not always merge with pre-existing PML NBs
371 (Supplemental movie 6). A possible interpretation of these observations will be presented
372 in the Discussion, but for now it can be concluded that these events are most easily explained
373 by a local and transient accumulation of IFI16 at viral genomes after their entry into the
374 nucleus, which is followed by a more stable recruitment of PML.

375 **Recruitment of hDaxx is detectable before that of PML**

376 The results of Figs. 5 and 6 suggest that hDaxx responds more quickly than PML to virus
377 infection, because there is a delay before the latter is detectable at the novel IFI16 foci, while
378 the former appears commonly within the same time frame. To test this directly, the relative
379 dynamics of recruitment of hDaxx and PML to HSV-1 induced foci were compared in HFs
380 constructed to express ECFP-hDaxx and EYFP-PML. A common phenomenon observed in
381 such cells near the periphery of developing ICP0-null mutant HSV-1 plaques was the
382 appearance of novel foci that first included hDaxx, then at a slightly later time PML was also
383 present. Many such examples are visible in the images of a time course presented in Fig. 7. A
384 longer period of the time course of this cell is shown in Supplemental movie 7. A detail of
385 one such example (boxed in the merged image of the first time point) is shown in the lowest
386 row of Fig 7. At the first time point, a dot which is green only is present, which at 15 minutes
387 is less intense (probably because it has moved slightly out of the focal plane) but by this time
388 it also includes PML. At the 35 min time point another new green dot has appeared at the
389 lower left of the detail (also clearly seen in the image of the whole cell nucleus; this also later
390 accumulates PML) while one of the pre-existing PML NBs has moved out of this segment,
391 leaving the dot that was green only at the start in the centre of detail. By the 45 min time
392 point this appears to merge with its nearest neighboring PML NB. Detailed examination of
393 the complete time course (see Supplemental movie 7) illustrates that these events are very
394 common in such cells; novel foci including only hDaxx appear, which later include both
395 hDaxx and PML, and which sometimes, but not always, merge with neighboring PML NBs.

396 Such events can only be detected by live cell analysis, which reveals these transient
397 and subtle events that occur in cells close to developing plaques. Previous examination of
398 such cells using fixed cell methods has concentrated on those in which marked viral genome
399 associated foci in arcs near the edge of the nucleus have been formed, because in these cases
400 it was clear that these novel foci were virus induced. The live cell analysis extends these
401 findings to reveal virus induced events in many cells that do not or have not yet formed the
402 characteristic peri-nuclear arcs of foci, and which could not be detected at such time points by
403 co-staining for ICP4.

404

405 **DISCUSSION**

406 The results presented in this paper allow an extension of previous models of the interactions
407 between HSV-1 genomes and PML NB proteins during the earliest stages of infection
408 (summarised in Fig. 8). At a very early stage of infection, probably within seconds and
409 certainly within minutes of the release of the viral genome through the nuclear pore into the
410 nucleoplasm, IFI16 can be seen to accumulate in distinct foci that are very likely to be closely
411 associated with the viral genomes. This event is PML independent, but it requires the pyrin
412 domain of IFI16 which is involved in its oligomerization on naked DNA (30). Equally
413 rapidly, hDaxx also accumulates in these foci, co-localizing with IFI16 transiently while after
414 a few minutes the IFI16 signal is dispersed. As the IFI16 signal weakens, PML then also
415 accumulates in the foci, co-localizing with hDaxx. All these events can be observed in both
416 wt and ICP0 null mutant infections, but in the latter the recruitment of hDaxx and PML is
417 much more difficult to detect because of the activity of ICP0 (9, 11, 13). In the absence of
418 ICP0, at high multiplicity and in cells which enter the lytic cycle, hDaxx and PML remain
419 associated at sites close to the viral genomes as replication compartments develop, and a
420 second and more stable phase of IFI16 recruitment occurs. At low multiplicity however, it is
421 known that the majority of ICP0 null mutant HSV-1 genomes are repressed. The evidence
422 here suggests that these genomes may remain stably associated with hDaxx and PML,
423 perhaps sequestered within these modified PML NB-like structures, which in some cases
424 appear to fuse with pre-existing PML NBs. This hypothesis is consistent with the observation
425 that quiescent HSV-1 genomes can be detected within enlarged PML NBs in fibroblasts (39)
426 (and in similar structures in latently infected mouse neurones; (40)). Unlike in the case of
427 active replication in which IFI16 more stably accumulates close to the viral genomes (Fig. 2),
428 IFI16 was not detected within PML NBs in quiescently infected cells (data not shown).
429 Therefore recruitment of IFI16 appears to be a transient event.

430 In previous studies on the recruitment of PML NB proteins to incoming HSV-1
431 genomes, the analysis has concentrated on cells in which there are abundant numbers of ICP4
432 foci close to the edge of the nucleus. This was because the asymmetric pattern of PML NB
433 protein foci could be clearly distinguished from their normal distribution in uninfected cells,
434 and therefore clear unequivocal conclusions could be made. The observation of virus induced
435 IFI16 foci in this study has allowed a more detailed analysis, because IFI16 never forms
436 small punctate foci in uninfected cells. The use of dual labelled cells, combining EYFP-IFI16
437 with either ECFP-hDaxx or ECFP-PML, also increases the compelling nature of the
438 observations. Because of these factors, the virus induced foci could be studied in cells in
439 which they are neither abundant nor routinely close to the nuclear envelope, within cells at the
440 early stages of a normal infection as well as of cells at the edges of developing plaques, and
441 also within a background of pre-existing PML NBs. The live cell sequences thus clearly show
442 the formation of novel virus-induced PML NB-like structures, that in some cases later fuse
443 with pre-existing PML NBs, events that could underlie the detection of multiple quiescent
444 viral genomes within enlarged PML NBs (39).

445 The mechanism of the recruitment of IFI16 to HSV-1 genomes involves several
446 factors. One important aspect is likely to be that at the point of delivery into the nucleoplasm
447 the viral DNA is not chromatinized, and this naked configuration is likely to underlie its
448 recognition by IFI16 (30). ChIP assays performed by others have confirmed a direct
449 association between IFI16 and HSV-1 DNA (25). IFI16 binds to DNA through its HIN
450 domains, and it can form oligomers on DNA through pyrin domain interactions (30). A single
451 HIN domain was sufficient for IFI16 to accumulate on HSV-1 genomes, and the pyrin domain
452 was essential for this abundant accumulation (Fig. 2). It is possible that the pyrin domain
453 mutant protein still binds to viral DNA, but lack of oligomerization may reduce its
454 accumulation on viral genomes to below a level detectable by microscopy. The recruitment of
455 several PML NB proteins to HSV-1 genomes occurs through SUMO-related pathways, but
456 whether sumoylation is also involved in the recruitment of IFI16 remains to be determined.
457 IFI16 has been identified as a substrate for sumoylation in proteomic screens (16, 41), but an
458 abundantly sumoylated form is not evident on western blots. Whatever the mechanisms
459 involved, they are clearly inhibited by ICP0. As abundant recruitment of IFI16 does not occur
460 in wt HSV-1 infected cells even when it remains easily detectable by fluorescence (24), this
461 inhibition is not a simple consequence of the degradation of IFI16 that occurs at later times of
462 wt HSV-1 infection (23, 24).

463 The transient nature of IFI16 accumulation in the virus induced foci is intriguing. It is
464 not a simple case of the entity in question moving out of focus (although this can occur),
465 because the hDaxx or PML signal remains. Clearly the recruitment of IFI16 is a very early
466 event, and it is possible that as the viral genome is assembled into more complex
467 nucleoprotein complexes, including nucleosomal structures, such that the parental viral DNA
468 ceases to be in a naked form required for IFI16 accumulation. The more stable accumulation
469 of IFI16 that occurs as replication compartments develop in ICP0 null mutant infections
470 could reflect the production of newly replicated naked DNA in these structures. However,
471 IFI16 does not co-localize with viral replication compartments in the same way as ICP8 and
472 ICP4 even in ICP0 null mutant infections, but instead it often forms tangled filament-like
473 structures that are associated with the replication compartments (24). These thread-like
474 structures are likely to represent oligomers of IFI16, but how they relate to the viral DNA
475 remains to be determined.

476 A fundamental question that is beyond the scope of this current study is whether or
477 not IFI16 plays an important role in the recruitment of other proteins to the HSV-1 genome.
478 This hypothesis would provide an interesting aspect to the role of IFI16 as a sensor of
479 pathogen DNA. Previously it was shown that in cells depleted of IFI16, the recruitment of
480 hDaxx appeared to be delayed, in that it was much more difficult to detect hDaxx in the
481 asymmetric staining pattern characteristic of infected cells prior to detectable expression of
482 ICP4 (in other words, cells of the phenotype of cell d in Fig. 1B were very rare in IFI16
483 depleted cells) (24). However, recruitment of both PML and hDaxx was readily detectable in
484 the majority of IFI16 depleted cells once ICP4 was expressed (24). Although depletion of
485 IFI16 was efficient in these cells, it is possible that trace remaining levels were sufficient for
486 a hypothetical function in which recruitment of IFI16 is a necessary step prior to recruitment
487 of the other proteins. Alternatively, the recruitment of IFI16 may be unlinked that that of
488 PML NB proteins, and is more involved in regulation of chromatin assembly on the viral
489 genome, as proposed by others (25, 26). Whatever the functions of the events described here,
490 it is clear that detailed examination in live cells reveals striking and unexpected aspects of the
491 dynamic nature of the interaction between cellular proteins and the invading HSV-1
492 genomes.

493

494 **FUNDING INFORMATION**

495 The work in the author's laboratory is funded by the Medical Research Council within the
496 University Unit of the MRC-University of Glasgow Centre for Virus Research (project

497 MC_UU_12014/4). The Zeiss Axio Observer Z1 microscopy system was purchased via a
498 grant from the Medical Research Foundation (grant reference C0446).

499

500 **ACKNOWLEDGEMENTS**

501 I am very grateful for the excellent technical assistance of Anne Orr, and I thank Jungsan
502 Sohn (IFI16 mutant m3), and Arkadiusz Welman and Margaret Frame (the GAPC vector) for
503 the indicated materials. The author would also like to acknowledge the many colleagues who
504 over the years have contributed to understanding of virus interactions with PML NBs,
505 particularly the late Gerd Maul who initiated this whole story.

506

507 **FIGURE LEGENDS**

508 **Figure 1**

509 Examples of recruitment of PML NB proteins to sites associated with HSV-1 genomes, as
510 detected by staining for ICP4. The panels show views of cells close to developing ICP0 null
511 mutant HSV-1 plaques in HFs, stained for ICP4 (green) and PML (red) (A) or ICP4 (green)
512 and hDaxx (red) (B). Cells indicated by 'a' show the pattern of PML or hDaxx expected of
513 uninfected cells. Cells labelled 'b' show various typical asymmetric patterns of ICP4 and
514 PML NB protein staining showing recruitment of PML or hDaxx to sites associated with
515 HSV-1 DNA. The cell labelled 'c' in (B) exhibits some faint foci of ICP4, each of which is
516 associated with hDaxx staining. The cell labelled 'd' in (B) shows a less common phenotype,
517 in which hDaxx foci are distributed in a highly asymmetric pattern, very likely associated
518 with parental HSV-1 genomes, but before ICP4 expression has reached a detectable level.

519

520 **Figure 2**

521 The PYD domain is required for the recruitment of IFI16 to HSV-1 genomes. A. A map of a
522 lentivirus vector that expresses EYFP-linked IFI16. B. Western blot analysis of cell extracts
523 from a cell line transduced with the vector, analysed for IFI16 (left) and EGFP (right). There
524 are three endogenous IFI16 isoforms, which differ in the number of 'S' regions in the hinge
525 region between Hin-200A and Hin-200B. Only a single EYFP-linked isoform is expressed in
526 these cells. C. A map of the coding sequence of IFI16, indicating the PYD and the two HIN
527 domains, with two linker sequences (S1, S2). Also marked are the locations of the triple point
528 mutations in mutant m3, and the region deleted in the mutant Δ HIN2. D. The nuclear
529 distribution of wild type (wt) and mutant m3 and Δ HIN2 mutant forms of IFI16, detected by
530 autofluorescence in transduced cell lines. E. The distributions of wt and mutant m3 and

531 Δ HIN2 mutant forms of IFI16 in cells at the edge of developing ICP0 null mutant plaques,
532 indicating prominent recruitment of wt and Δ HIN2 IFI16, but not the m3 mutant, to sites that
533 are closely associated with HSV-1 genomes (detected by staining for ICP4). F. Depletion of
534 PML does not compromise efficient recruitment of IFI16 to HSV-1 genomes. The panels
535 show either uninfected HFs or examples of cells at the edge of ICP0 null mutant HSV-1
536 plaques stained for hDaxx and IFI16, in control and PML depleted cells (left- and right-hand
537 pairs of images, respectively).

538

539 **Figure 3**

540 Detection of the rapid response of IFI16 to HSV-1 infection. A. HFs expressing EYFP-IFI16
541 were infected with ICP0 null mutant HSV-1 (MOI 50) then images were captured at the
542 indicated times after addition of the virus. B. A similar experiment was conducted using wt
543 HSV-1 infection (MOI 20). C. Images from a sequence of a cell close to the edge of an ICP0
544 null mutant HSV-1 plaque. D. HFs expressing EYFP-IFI16 were infected with virus dl0C4
545 and images from a sequence of a cell at the edge of a developing plaque are presented,
546 showing the IFI16, ICP4 and merged signals as indicated.

547

548 **Figure 4**

549 Dynamics of PML.I and hDaxx in uninfected cells and their rapid recruitment to sites
550 associated with HSV-1 genomes. (A). Uninfected HepaRG cells transduced to express either
551 GAPC-PML.I or GAPC-hDaxx were imaged before and after photoactivation of the PA-
552 EGFP moiety within the red boxed area. Detection of PA-EGFP at intervals after
553 photoactivation reveals migration of activated molecules from the activated region to the rest
554 of the nucleoplasm. (B). As for A, but cells at the edge of developing ICP0 mutant HSV-1
555 plaques with characteristic asymmetrically distributed foci were examined under the same
556 activation and time course conditions. Activated hDaxx can be detected in the asymmetric
557 foci at the first time point after bleaching (about 2 seconds), becoming more prominent as
558 time progresses. Activated PML accumulates in the foci at the nuclear periphery more
559 slowly.

560

561 **Figure 5**

562 IFI16 and hDaxx respond to HSV-1 infection with similar kinetics. HFs expressing EYFP-
563 IFI16 and ECFP-hDaxx were infected with ICP0 null mutant HSV-1 (MOI 100). After a 15
564 minute absorption period, the cells were examined by live cell microscopy, with images

565 captured every 90 sec. A selection of images is shown, with the times after adding the virus
566 indicated in the top row. The upper three rows show the IFI16, hDaxx and merged channels,
567 with the numbered arrows pointing to IFI16 foci that transiently appear during the sequence.
568 The corresponding foci are also indicated on the hDaxx and merged panels. The sets of
569 smaller images show details from each time point of the boxed areas marked in the 48 min
570 sample. The left- and right-hand columns of these images for each time point show the
571 images corresponding to the lower and upper boxes respectively, using the same numbering
572 system. In this sequence covering just 9 minutes, four IFI16 foci appear simultaneously with
573 an hDaxx signal, although in dot 3 the latter is weak at the 55.5 min time point. The presence
574 of IFI16 is transient in dots 1 and 2 in this sequence, while hDaxx is more stable. A longer
575 sequence from the same time course is shown in Supplemental movie 5, in which several
576 other examples of the same phenomena can be seen.

577

578 **Figure 6**

579 IFI16 responds to HSV-1 infection more rapidly than PML. HF's expressing EYFP-IFI16 and
580 ECFP-PML were infected with ICP0 null mutant HSV-1 (MOI 25). After a 20 minute
581 absorption period, the cells were examined by live cell microscopy, with images captured
582 every minute, starting 35 min after addition of the virus. A selection of images from the time
583 course are presented, showing a cell in which a novel focus of IFI16 appears, which later
584 becomes PML positive before merging with a pre-existing PML NB structure. The lower set
585 of three rows presents expansions for each time point of the boxed area in the merged image of
586 the 82 min time point. Further details are provided in the text.

587

588 **Figure 7**

589 hDaxx responds more rapidly than PML to HSV-1 infection. HF's expressing both ECFP-
590 hDaxx and EYFP-PML were infected with ICP0-null mutant HSV-1 and cells at the edge of a
591 developing plaque were examined. A selection of images from an image sequence are
592 presented, indicating the time (arbitrary) after the first image shown (which is image 54 of the
593 original sequence, frame 24 as presented in Supplemental movie 7). The lowermost row
594 shows a magnified view of the region that is boxed in the merged image of the leftmost
595 column. Further details are provided in the text.

596

597

598

599 **Figure 8**

600 A model for the dynamics of IFI16 and PML NB components to HSV-1 genomes. A full
601 explanation is provided in the text. The hexagon on the left represents a full capsid bound to
602 the outer side of a nuclear pore through which the naked viral genome (tangled line) is
603 transferred into the nucleoplasm.

604

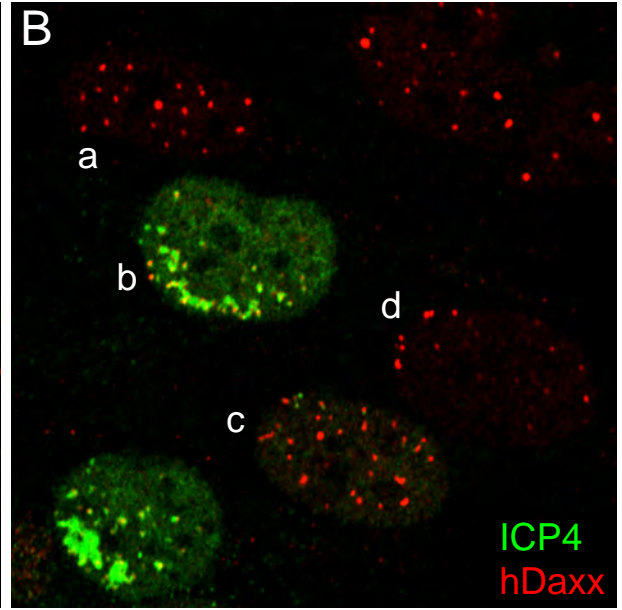
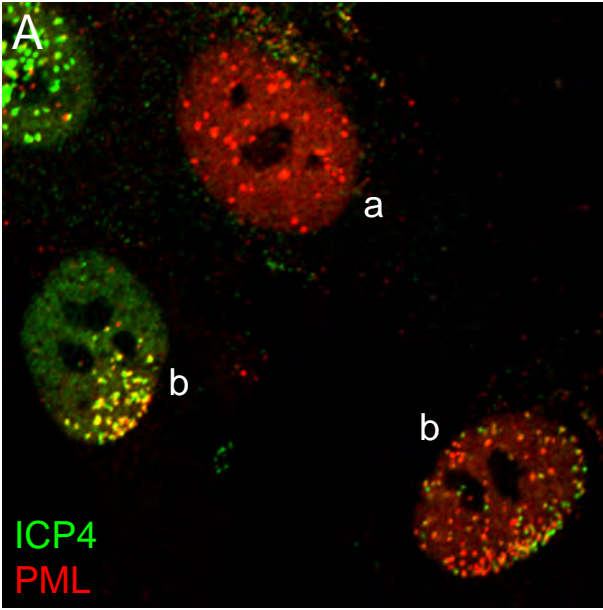
605 **REFERENCES**

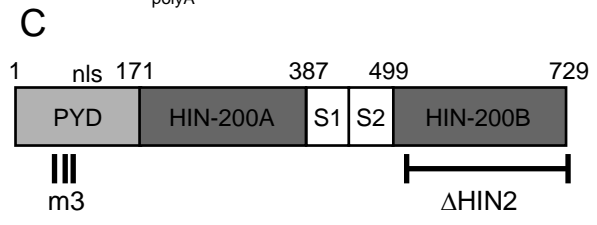
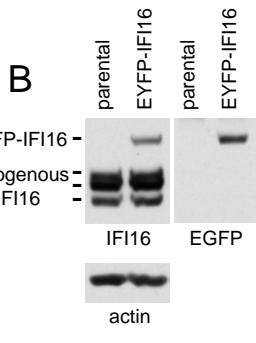
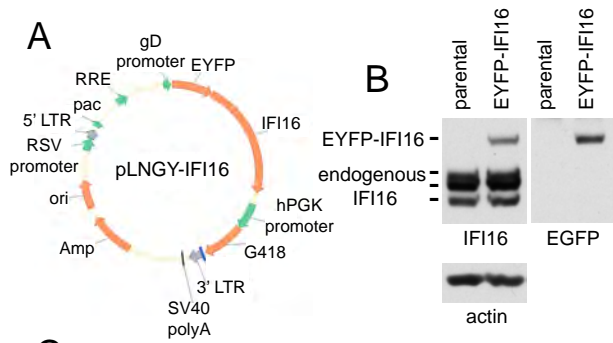
- 606 1. **Boutell C, Everett RD.** 2013. Regulation of alphaherpesvirus infections by the ICP0
607 family of proteins. *J Gen Virol* **94**:465-481.
- 608 2. **Geoffroy MC, Chelbi-Alix MK.** 2011. Role of promyelocytic leukemia protein in
609 host antiviral defense. *J Interferon Cytokine Res* **31**:145-158.
- 610 3. **Tavalai N, Stamminger T.** 2008. New insights into the role of the subnuclear
611 structure ND10 for viral infection. *Biochim Biophys Acta* **1783**:2207-2221.
- 612 4. **Everett RD, Boutell C, Orr A.** 2004. Phenotype of a herpes simplex virus type 1
613 mutant that fails to express immediate-early regulatory protein ICP0. *J Virol* **78**:1763-
614 1774.
- 615 5. **Stow ND, Stow EC.** 1986. Isolation and characterization of a herpes simplex virus
616 type 1 mutant containing a deletion within the gene encoding the immediate early
617 polypeptide Vmw110. *J Gen Virol* **67**:2571-2585.
- 618 6. **Yao F, Schaffer PA.** 1995. An activity specified by the osteosarcoma line U2OS can
619 substitute functionally for ICP0, a major regulatory protein of herpes simplex virus
620 type 1. *J Virol* **69**:6249-6258.
- 621 7. **Everett RD, Parada C, Gripon P, Sirma H, Orr A.** 2008. Replication of ICP0-null
622 mutant herpes simplex virus type 1 is restricted by both PML and Sp100. *J Virol*
623 **82**:2661-2672.
- 624 8. **Everett RD, Rechter S, Papior P, Tavalai N, Stamminger T, Orr A.** 2006. PML
625 contributes to a cellular mechanism of repression of herpes simplex virus type 1
626 infection that is inactivated by ICP0. *J Virol* **80**:7995-8005.
- 627 9. **Lukashchuk V, Everett RD.** 2010. Regulation of ICP0-null mutant herpes simplex
628 virus type 1 infection by ND10 components ATRX and hDaxx. *J Virol* **84**:4026-4040.
- 629 10. **Glass M, Everett RD.** 2013. Components of promyelocytic leukemia nuclear bodies
630 (ND10) act cooperatively to repress herpesvirus infection. *J Virol* **87**:2174-2185.

- 631 11. **Everett RD, Murray J.** 2005. ND10 components relocate to sites associated with
632 herpes simplex virus type 1 nucleoprotein complexes during virus infection. *J Virol*
633 **79**:5078-5089.
- 634 12. **Lukashchuk V, Orr A, Everett RD.** 2010. Regulation of ICP0 null mutant HSV-1
635 infection by ND10 components ATRX and hDaxx. *J Virol* **84**:4026-4040.
- 636 13. **Cuchet-Lourenco D, Boutell C, Lukashchuk V, Grant K, Sykes A, Murray J,**
637 **Orr A, Everett RD.** 2011. SUMO pathway dependent recruitment of cellular
638 repressors to herpes simplex virus type 1 genomes. *PLoS Pathog* **7**:e1002123.
- 639 14. **Boutell C, Cuchet-Lourenco D, Vanni E, Orr A, Glass M, McFarlane S, Everett**
640 **RD.** 2011. A viral ubiquitin ligase has substrate preferential SUMO targeted ubiquitin
641 ligase activity that counteracts intrinsic antiviral defence. *PLoS Pathog* **7**:e1002245.
- 642 15. **Everett RD, Freemont P, Saitoh H, Dasso M, Orr A, Kathoria M, Parkinson J.**
643 1998. The disruption of ND10 during herpes simplex virus infection correlates with
644 the Vmw110- and proteasome-dependent loss of several PML isoforms. *J Virol*
645 **72**:6581-6591.
- 646 16. **Sloan E, Tatham MH, Gros Lambert M, Glass M, Orr A, Hay RT, Everett RD.**
647 2015. Analysis of the SUMO2 Proteome during HSV-1 Infection. *PLoS Pathog*
648 **11**:e1005059.
- 649 17. **Ishov AM, Sotnikov AG, Negorev D, Vladimirova OV, Neff N, Kamitani T, Yeh**
650 **ET, Strauss JF, 3rd, Maul GG.** 1999. PML is critical for ND10 formation and
651 recruits the PML-interacting protein daxx to this nuclear structure when modified by
652 SUMO-1. *J Cell Biol* **147**:221-234.
- 653 18. **Zhong S, Muller S, Ronchetti S, Freemont PS, Dejean A, Pandolfi PP.** 2000. Role
654 of SUMO-1-modified PML in nuclear body formation. *Blood* **95**:2748-2752.
- 655 19. **Cuchet D, Sykes A, Nicolas A, Orr A, Murray J, Sirma H, Heeren J, Bartelt A,**
656 **Everett RD.** 2011. PML isoforms I and II participate in PML-dependent restriction of
657 HSV-1 replication. *J Cell Sci* **124**:280-291.
- 658 20. **Lilley CE, Chaurushiya MS, Boutell C, Everett RD, Weitzman MD.** 2011. The
659 intrinsic antiviral defense to incoming HSV-1 genomes includes specific DNA repair
660 proteins and is counteracted by the viral protein ICP0. *PLoS Pathog* **7**:e1002084.
- 661 21. **Unterholzner L, Bowie AG.** 2011. Innate DNA sensing moves to the nucleus. *Cell*
662 *Host Microbe* **9**:351-353.

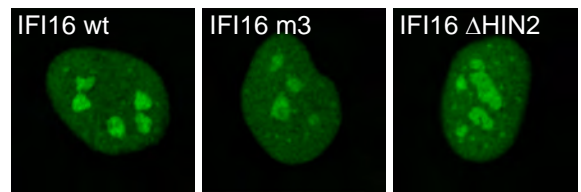
- 663 22. **Unterholzner L, Keating SE, Baran M, Horan KA, Jensen SB, Sharma S, Sirois**
664 **CM, Jin T, Latz E, Xiao TS, Fitzgerald KA, Paludan SR, Bowie AG.** 2010. IFI16
665 is an innate immune sensor for intracellular DNA. *Nat Immunol* **11**:997-1004.
- 666 23. **Orzalli MH, DeLuca NA, Knipe DM.** 2012. Nuclear IFI16 induction of IRF-3
667 signaling during herpesviral infection and degradation of IFI16 by the viral ICP0
668 protein. *Proc Natl Acad Sci U S A* **109**:E3008-3017.
- 669 24. **Cuchet-Lourenco D, Anderson G, Sloan E, Orr A, Everett RD.** 2013. The viral
670 ubiquitin ligase ICP0 is neither sufficient nor necessary for degradation of the cellular
671 DNA sensor IFI16 during herpes simplex virus 1 infection. *J Virol* **87**:13422-13432.
- 672 25. **Johnson KE, Bottero V, Flaherty S, Dutta S, Singh VV, Chandran B.** 2014. IFI16
673 restricts HSV-1 replication by accumulating on the hsv-1 genome, repressing HSV-1
674 gene expression, and directly or indirectly modulating histone modifications. *PLoS*
675 *Pathog* **10**:e1004503.
- 676 26. **Orzalli MH, Conwell SE, Berrios C, DeCaprio JA, Knipe DM.** 2013. Nuclear
677 interferon-inducible protein 16 promotes silencing of herpesviral and transfected
678 DNA. *Proc Natl Acad Sci U S A* **110**:E4492-4501.
- 679 27. **Orzalli MH, Broekema NM, Diner BA, Hancks DC, Elde NC, Cristea IM, Knipe**
680 **DM.** 2015. cGAS-mediated stabilization of IFI16 promotes innate signaling during
681 herpes simplex virus infection. *Proc Natl Acad Sci U S A* **112**:E1773-1781.
- 682 28. **Diner BA, Lum KK, Javitt A, Cristea IM.** 2015. Interactions of the antiviral factor
683 IFI16 mediate immune signaling and herpes simplex virus-1 immunosuppression. *Mol*
684 *Cell Proteomics*.
- 685 29. **Li T, Diner BA, Chen J, Cristea IM.** 2012. Acetylation modulates cellular
686 distribution and DNA sensing ability of interferon-inducible protein IFI16. *Proc Natl*
687 *Acad Sci U S A* **109**:10558-10563.
- 688 30. **Morrone SR, Wang T, Constantoulakis LM, Hooy RM, Delannoy MJ, Sohn J.**
689 2014. Cooperative assembly of IFI16 filaments on dsDNA provides insights into host
690 defense strategy. *Proc Natl Acad Sci U S A* **111**:E62-71.
- 691 31. **Welman A, Serrels A, Brunton VG, Ditzel M, Frame MC.** 2010. Two-color
692 photoactivatable probe for selective tracking of proteins and cells. *J Biol Chem*
693 **285**:11607-11616.
- 694 32. **Stuurman N, de Graaf A, Floore A, Josso A, Humbel B, de Jong L, van Driel R.**
695 1992. A monoclonal antibody recognizing nuclear matrix-associated nuclear bodies. *J*
696 *Cell Sci* **101**:773-784.

- 697 33. **Showalter SD, Zweig M, Hampar B.** 1981. Monoclonal antibodies to herpes
698 simplex virus type 1 proteins, including the immediate-early protein ICP 4. *Infect*
699 *Immun* **34**:684-692.
- 700 34. **Ishov AM, Maul GG.** 1996. The periphery of nuclear domain 10 (ND10) as site of
701 DNA virus deposition. *J Cell Biol* **134**:815-826.
- 702 35. **Maul GG, Ishov AM, Everett RD.** 1996. Nuclear domain 10 as preexisting potential
703 replication start sites of herpes simplex virus type-1. *Virology* **217**:67-75.
- 704 36. **Brand P, Lenser T, Hemmerich P.** 2010. Assembly dynamics of PML nuclear
705 bodies in living cells. *PMC Biophys* **3**:3.
- 706 37. **Weidtkamp-Peters S, Lenser T, Negorev D, Gerstner N, Hofmann TG,**
707 **Schwanitz G, Hoischen C, Maul G, Dittrich P, Hemmerich P.** 2008. Dynamics of
708 component exchange at PML nuclear bodies. *J Cell Sci* **121**:2731-2743.
- 709 38. **Wiesmeijer K, Molenaar C, Bekeer IM, Tanke HJ, Dirks RW.** 2002. Mobile foci
710 of Sp100 do not contain PML: PML bodies are immobile but PML and Sp100
711 proteins are not. *J Struct Biol* **140**:180-188.
- 712 39. **Everett RD, Murray J, Orr A, Preston CM.** 2007. Herpes simplex virus type 1
713 genomes are associated with ND10 nuclear substructures in quiescently infected
714 human fibroblasts. *J Virol* **81**:10991-11004.
- 715 40. **Catez F, Picard C, Held K, Gross S, Rousseau A, Theil D, Sawtell N, Labetoulle**
716 **M, Lomonte P.** 2012. HSV-1 genome subnuclear positioning and associations with
717 host-cell PML-NBs and centromeres regulate LAT locus transcription during latency
718 in neurons. *PLoS Pathog* **8**:e1002852.
- 719 41. **Tammsalu T, Matic I, Jaffray EG, Ibrahim AF, Tatham MH, Hay RT.** 2014.
720 Proteome-Wide Identification of SUMO2 Modification Sites. *Sci Signal* **7**:rs2.
721

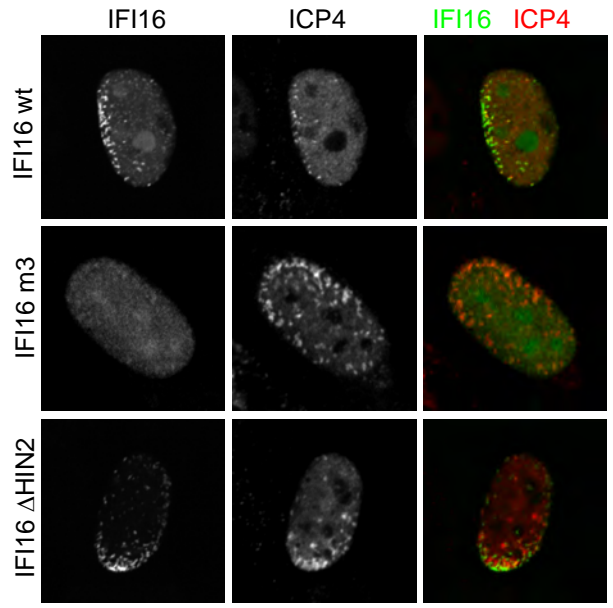




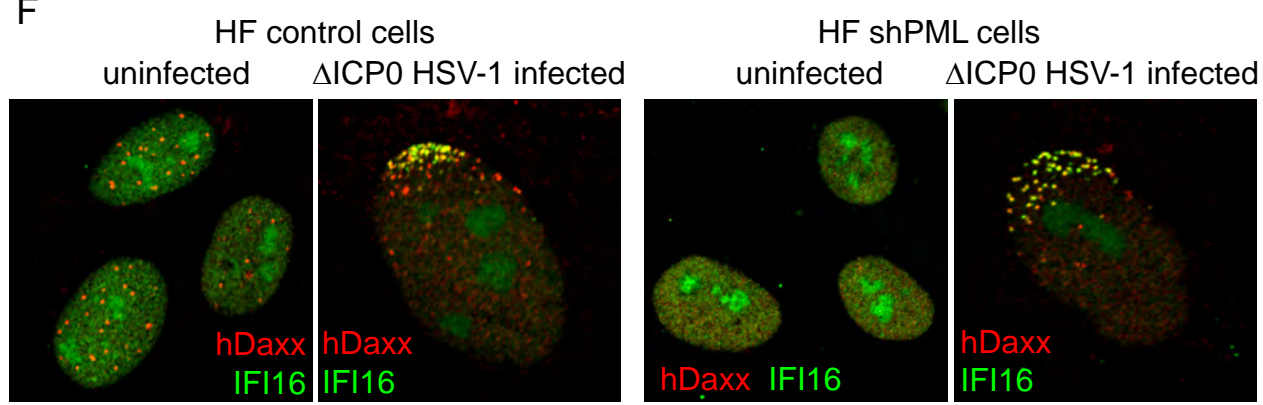
D uninfected cells



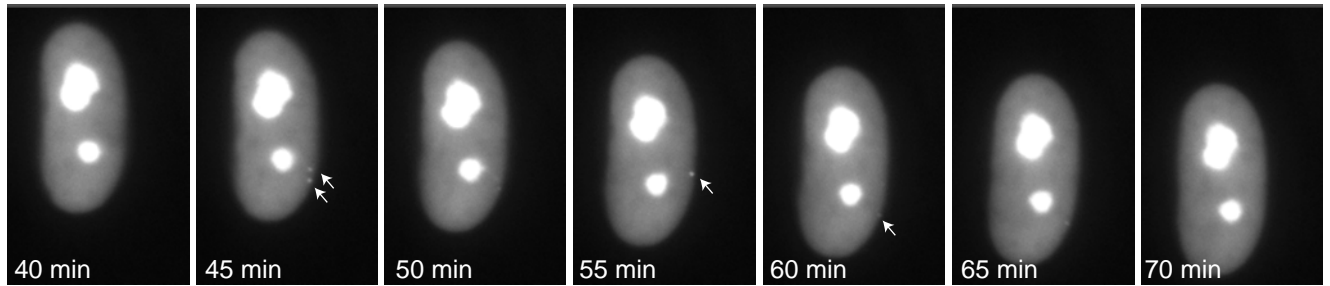
E ΔICP0 mutant infected cells



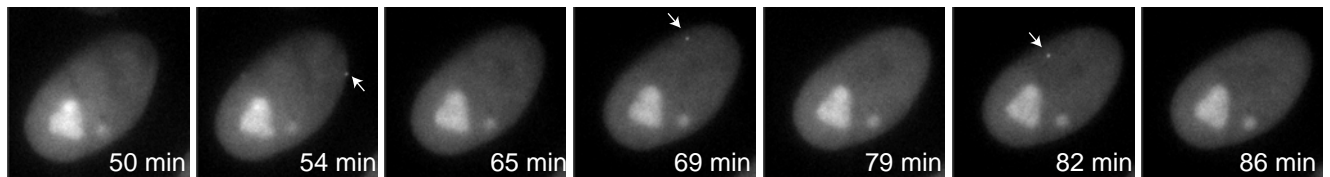
F



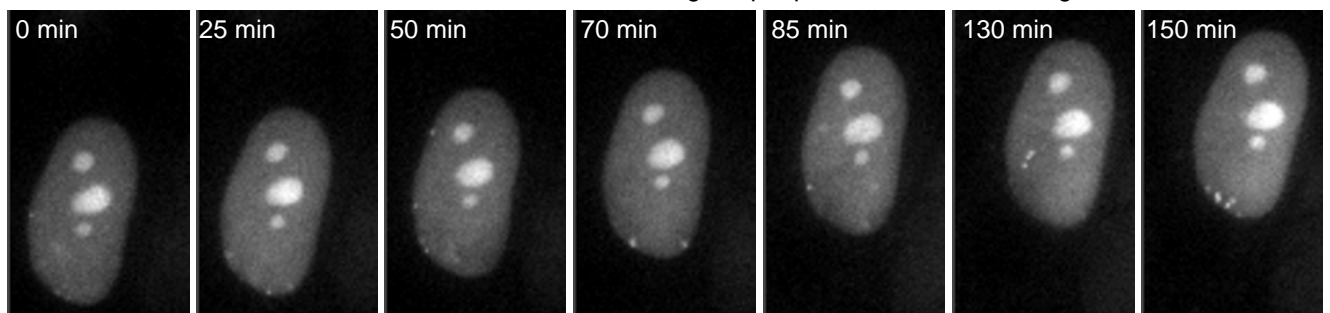
A: HF_s, EYFP-IFI16, infected with Δ ICP0 HSV-1, times after addition of virus



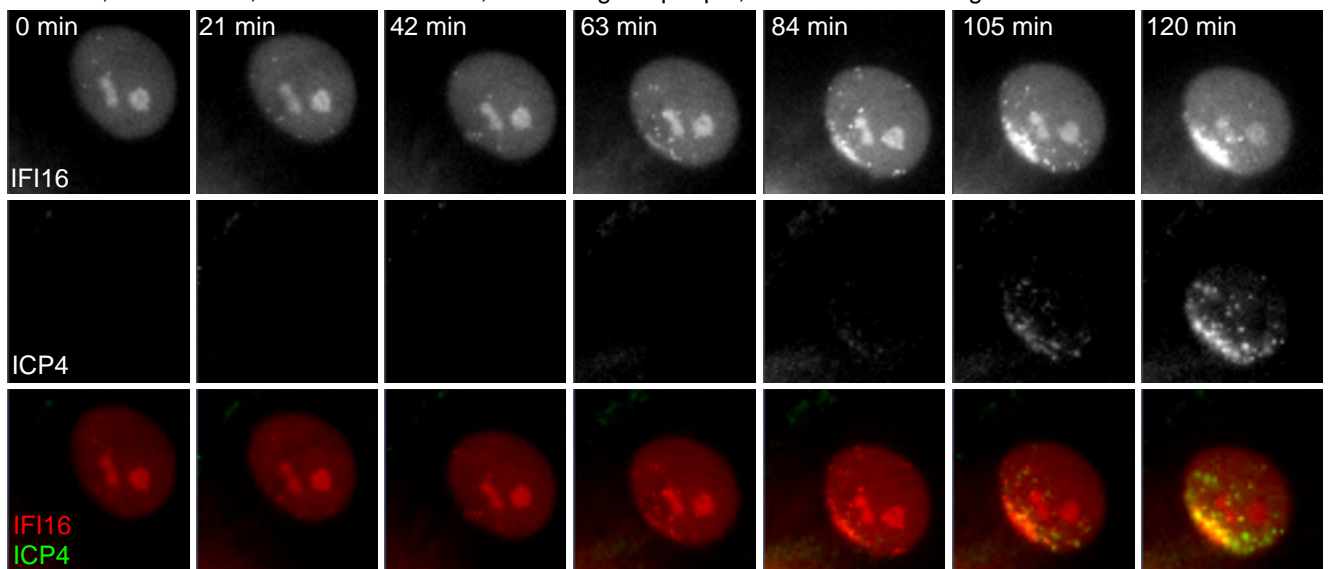
B: HF_s, EYFP-IFI16, infected with wt HSV-1, times after addition of virus



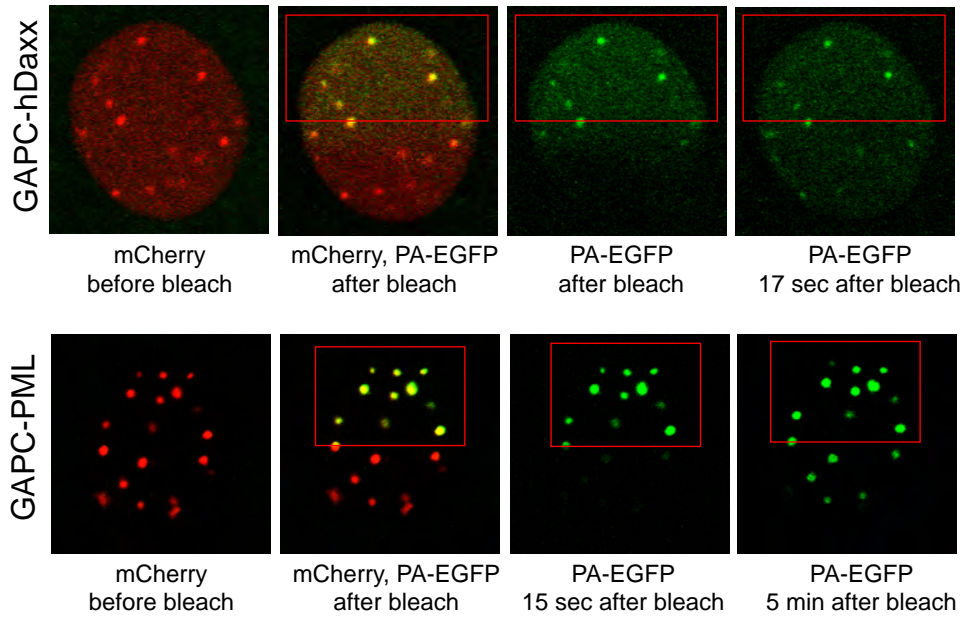
C: HF_s, EYFP-IFI16, infected with Δ ICP0 HSV-1, cell at edge of plaque, times after first image



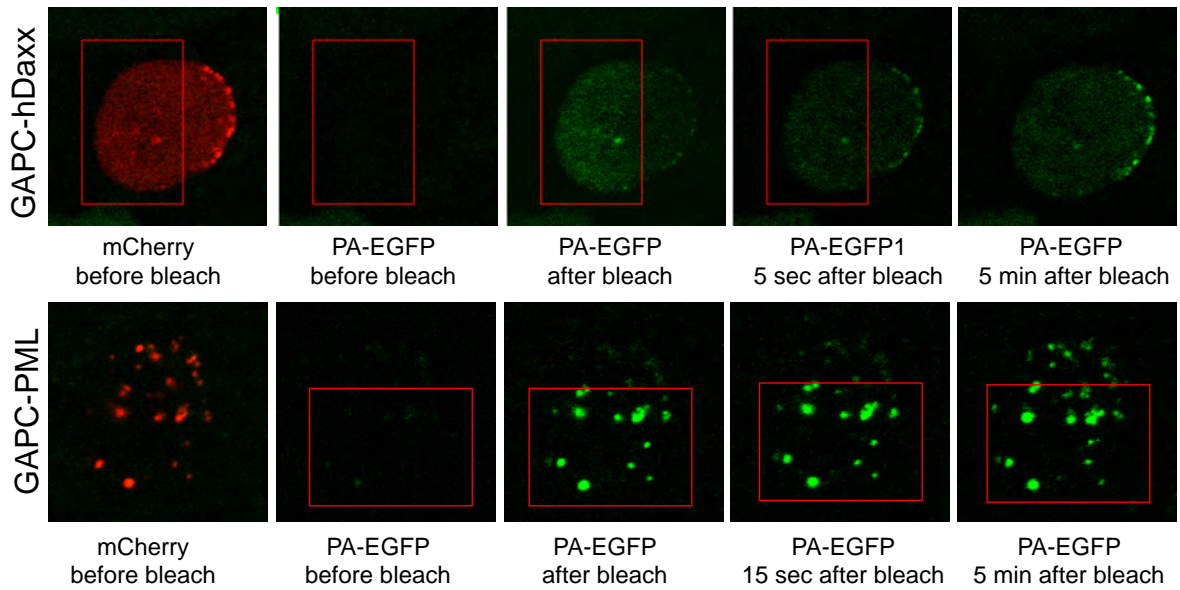
D: HF_s, EYFP-IFI16, infected with dl0C4, cell at edge of plaque, times after first image



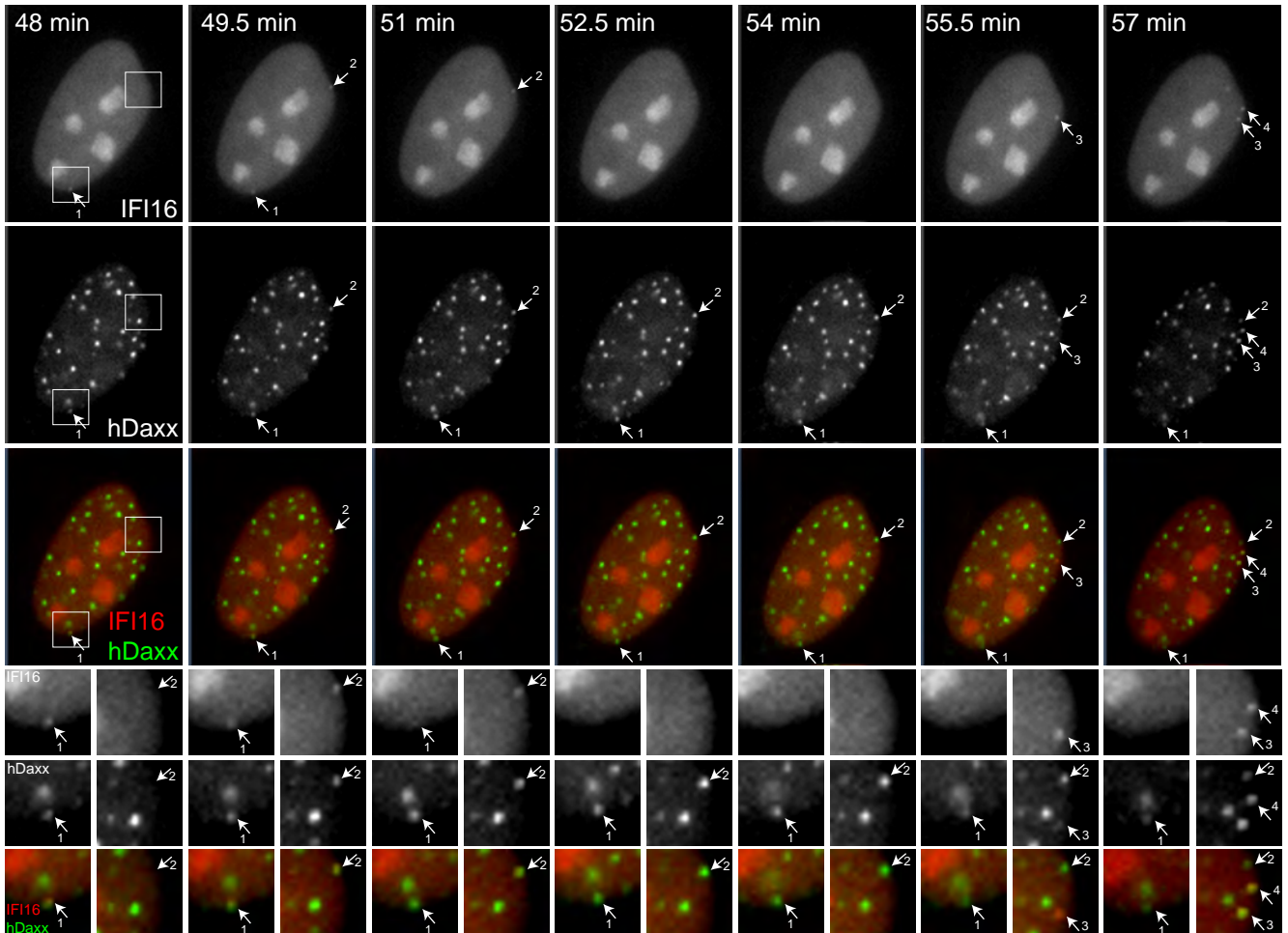
A. Uninfected cells



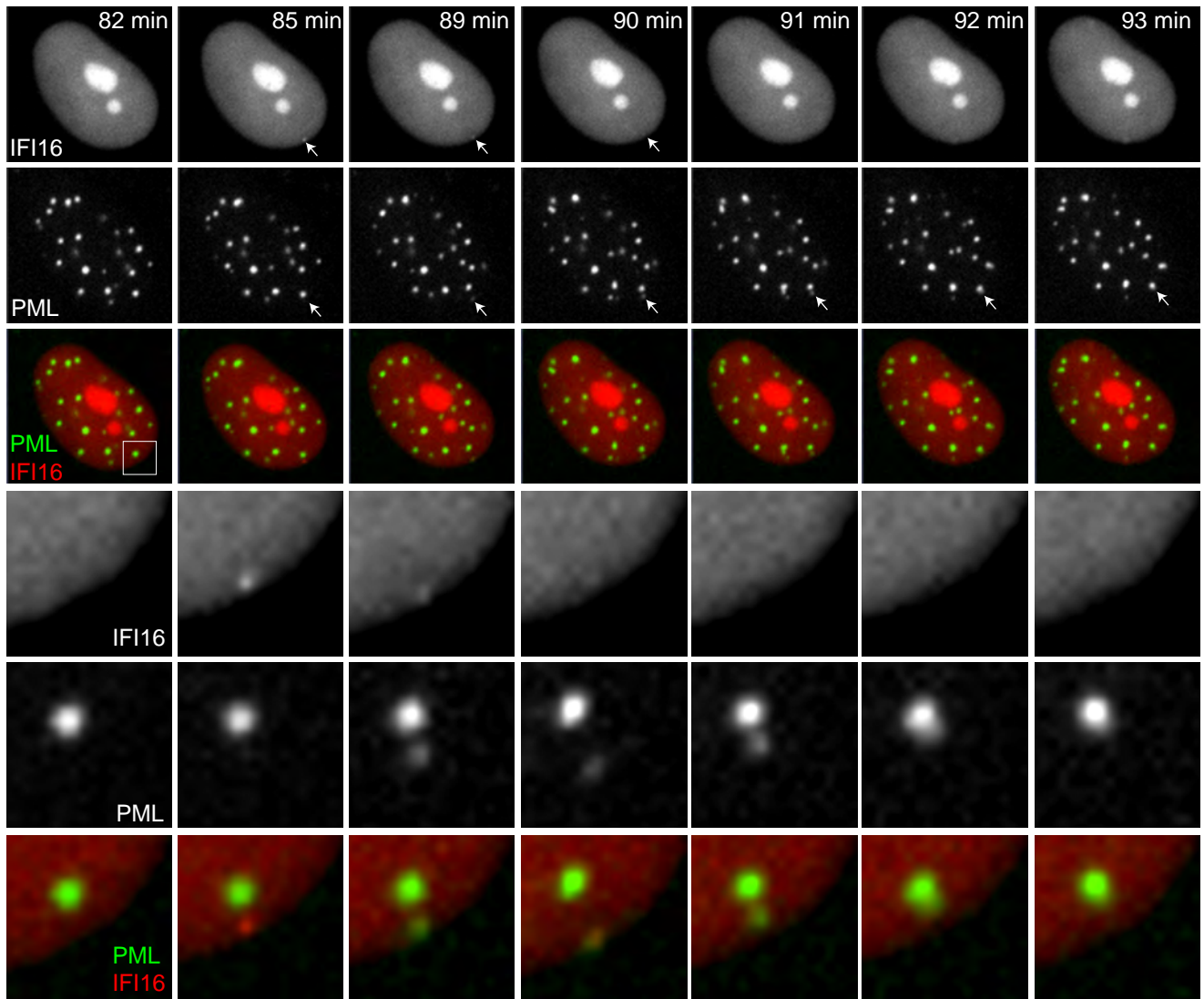
B. Δ ICP0 HSV-1 infected cells, edge of developing plaque



HFs, EYFP-IFI16 and ECFP-hDaxx, infected with Δ ICP0 HSV-1 (MOI 100), times after addition of virus



HF, EYFP-IFI16 and ECFP-PML, infected with Δ ICP0 HSV-1 (MOI 25), times after addition of virus



HF, ECFP-hDaxx and EYFP-PML, infected with Δ ICP0 HSV-1, cell at edge of plaque, times after first image

